Laser-conditioning mechanism of ZrO_2/SiO_2 HR films with fitting damage probability curves of laser-induced damage

Xiao Li (李 笑)[1,2*], Xiaofeng Liu (刘晓凤)[1,2], Yuan'an Zhao (赵元安)[1], Jianda Shao (邵建达)[1], and Zhengxiu Fan (范正修)[1]

[1]*Key Laboratory of High Power Laser Material, Shanghai Institute of Optics and Fine Mechanics, Chinese Academy of Sciences, Shanghai 201800, China*

[2]*Graduate University of Chinese Academy of Sciences, Beijing 100049, China*

[*]*E-mail: sanxiaoli@siom.ac.cn*

Received December 4, 2009

The method of fitting damage probability curves of laser-induced damage is introduced to investigate the laser-conditioning mechanism of ZrO_2/SiO_2 high reflection (HR) films. The laser-induced damage thresholds (LIDTs) of the sample are tested before and after the laser-conditioning scanning process. The parameters of the defects are obtained through the fitting process of the damage probability curve. It can be concluded that the roles of laser conditioning include two aspects: removing defects with lower threshold and producing new defects with higher threshold. The effect of laser conditioning is dependent on the competition of these two aspects.

OCIS codes: 140.3330, 310.6870.

doi: 10.3788/COL20100806.0598.

Many researchers use laser conditioning to increase the damage threshold of optical components[1−11]. Several laser-conditioning mechanisms such as laser cleaning[3], electronic defect model[7], and defect removal model[8] have been proposed. In most cases, defects in the surface of the material and in the bulk have been considered as playing a dominant role in laser-induced damage, as well as in the laser-conditioning process[12,13]. There are two methods to obtain the information of the defects. One is to obtain the characteristics of initiation defects utilizing the spot size effect of laser-induced damage[13]. Assuming that the initiations in the film in the same threshold are similar, the characteristics of the defect threshold and the densities of initiation defects could be obtained. Finally, several kinds of initiation defects also simultaneously serve as damage sources. Therefore, the ensemble of the defects needs to be determined.

Another way to obtain information regarding the defects is to plot laser-damage probability curves[14,15] in order to provide the ensemble of the defects in the film. Several models have been developed to interpret laser-damage probability curves, which involve parameters such as the nano-precursor threshold and their density[16−18]. The model assumes that the defects cause the damage according to a power law. A three-parameter damage probability law considered is therefore a better model. The model provides the information about the shape of the defect ensemble, in addition to the damage threshold and the defect density. This model has been investigated by Krol *et al.*[14,15], while considering a Gaussian distribution of nano-precursor thresholds. They proposed a Gaussian law and gave the parameters of the distribution, such as threshold mean value T_0, threshold standard deviation ΔT, and precursor defect densities d, for each kind of observed precursor. They also proposed the defect ensemble function $g(T)$ to represent the density of defect initiating damage at fluence T. The probability of damage at fluence F is expressed as

$$P(F) = 1 - \exp\left\{ -\frac{\sqrt{\pi} d\omega^2}{\Delta T\sqrt{2}} \times \int_0^F \exp\left[-\frac{1}{2}(\frac{T-T_0}{\Delta T/2})^2\right] \ln(\frac{F}{T})\mathrm{d}T \right\}, \quad (1)$$

$$g(T) = \frac{2d}{\Delta T\sqrt{2\pi}} \exp\left[-\frac{1}{2}\left(\frac{T-T_0}{\Delta T/2}\right)^2\right], \quad (2)$$

where ω is the spot diameter defined at $1/e^2$.

Equation (1) is used to fit the experimental data by using standard deviation σ^2 as an objective function:

$$\sigma^2 = \frac{\sum_{i=1}^{n} (P_{fi} - P_{ei})^2}{n}, \quad (3)$$

where P_{fi} is the damage probability in Eq. (1), P_{ei} is the corresponding damage probability tested, and n is the number of damage probabilities tested. The value of σ^2 is obtained by changing the parameters. Parameters such as T_0, ΔT, and d indicate the defects when the value of σ^2 is the smallest. Then, the damage precursor ensemble function is obtained using Eq. (2).

In this letter, the laser conditioning of ZrO_2/SiO_2 high reflection (HR) films at 1064-nm wavelength prepared by electron-beam evaporation on K9 glass substrates is reported. In addition, the transformation of the defects is analyzed by fitting the damage probability curves of laser-induced damage. The film stacks adopted was G|HL(2H2L)^{15}2H|A, where G is the substrate K9 glass, H is the HR material ZrO_2, L is the low reflective material SiO_2, and A is the incident medium air. Figure 1 shows the transmittance of the sample. The wavelength of the laser pulse used in the laser-induced damage

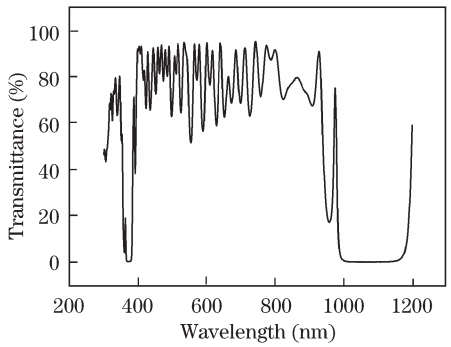

Fig. 1. Transmittance of the sample.

test and the laser-conditioning process was 1064 nm, while its pulse duration was 12 ns. Traditionally, the one-on-one laser-induced damage threshold (LIDT) tests are conducted under one selected laser spot size according to ISO11254[19], which is the standard of LIDT of laser-induced damage threshold of optical surfaces to determine their LIDTs. The experimental setup was built, and is shown schematically in Fig. 2.

The output pulse of the Nd:YAG laser system was 1064 nm with a pulse width of 12 ns. The laser was focused on the target normally using a lens. The spot size of the Gaussian diameter was 300 μm, measured using the knife method. The attenuator and a half-wave plate were employed to adjust the pulse energy radiating the sample. The sample was mounted normally to the beam on a step motor, which was used to position different test sites. Online imaging system of 200 magnifications comprising a charge-coupled device and a microscope was used to observe the radiating area and check whether the damage occurs during the one-on-one damage test and the laser-conditioning scanning process.

We conducted one-on-one damage tests before laser conditioning. Ten sites on the sample surface were tested with the same pulse energy, and the fraction of damage was recorded. This procedure was repeated for different pulse energies until it was sufficiently broad to include points with 0 and 100% damage probabilities. Data on laser energy density and the corresponding damage probabilities were obtained. The fitting process of defects in the films was conducted using Eq. (1) to obtain the characteristics of the initiation defects, including T_0, ΔT, and d. Then, the laser-conditioning process was conducted with a laser energy density selected according to the characteristics of the defects. The small spot-scanning process was employed to laser-condition the samples. The schematic is shown in Fig. 3. The sample was moved a certain distance after one shot of laser irradiation. Then, the second zone received the laser radiation, and so on. The scanning spot diameter adopted was 650 μm. The scanning step length was 300 μm, which is a little shorter than half of the laser spot diameter. A square zone of 12 ×12 (cm) was laser-conditioned for approximately 1 h. Then, the one-on-one damage tests were conducted at the conditioned zone to obtain data on laser energy density and the corresponding damage probabilities after laser conditioning. We obtained the characteristics of the defects in the films after laser conditioning using a similar method. It was then possible to obtain the ensemble functions of the defects before and after laser conditioning and compare the change of the ensemble of the defects.

The results of LIDT before and after laser conditioning were 12.7 and 25.3 J/cm^2, respectively, indicating that the LIDT increasing factor is approximately 2.0. The damage probability curves before and after laser conditioning were obtained by fitting the damage data tested using the damage probability formula by changing the parameters such as T_0, ΔT, and d, and with the smallest σ^2 as the objective function. These probability curves are shown in Fig. 4, while the obtained fitting parameters

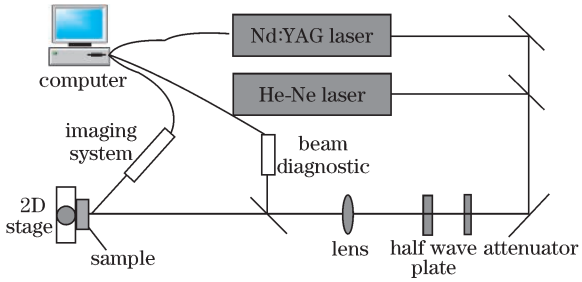

Fig. 2. Experimental setup. 2D: two-dimensional.

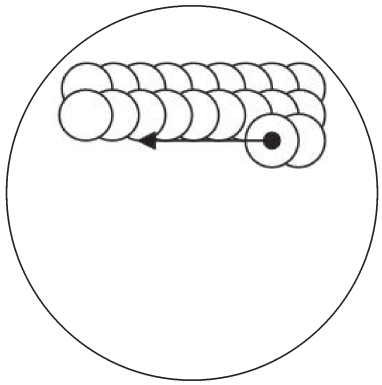

Fig. 3. Scanning process.

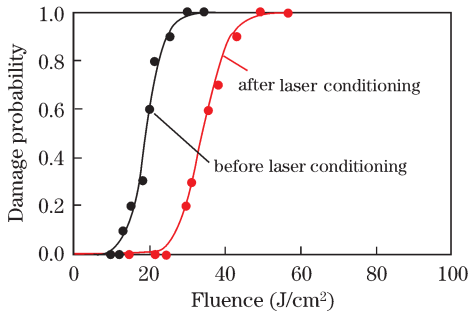

Fig. 4. Comparison of fitting of damage probability before and after laser conditioning.

Table 1. Fitting Parameters Obtained from the Best Fitting

	T_0 (J/cm^2)	ΔT (J/cm^2)	d (cm^2)
Before Laser Conditioning	21.0	9.0	1.7×10^3
After Laser Conditioning	36.0	12.0	2.1×10^3

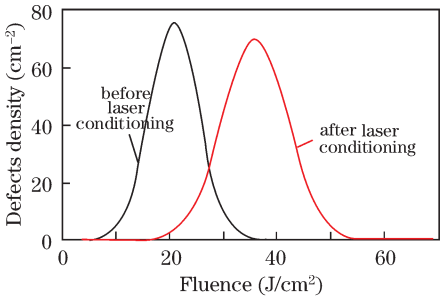

Fig. 5. Comparison of $g(T)$ curves before and after laser conditioning.

are listed in Table 1.

Table 1 shows that the average threshold of the defects in the film increases from 21.0 to 36.0 J/cm^2. The defect density increases from 1.7×10^3 to 2.1×10^3 cm^{-2}. Figure 4 shows that the damage probability decreases after laser conditioning at the same energy density below 100% damage probability. For example, the damage probabilities at the laser energy density of 20 J/cm^2 were approximately 20% and approximately 0 before and after laser conditioning, respectively. Therefore, it is proven that resistance to laser-induced damage in the film is increased by laser conditioning. The increased threshold is attributed to two aspects. One is that the defects with lower threshold are removed from the film, while the defects with higher threshold are not transformed to be defects with lower threshold. Additionally, the defects with higher threshold could be partially removed from the film. The other is that the lower threshold is partially removed from the film and then partially transformed into defects with higher threshold. In the former, the density of defects should be decreased because some defects are removed from the film. However, the defect density increases after laser conditioning. This indicates that the latter should be the laser-conditioning effect, or indicates that new defects should be produced. This could be interpreted by the ensemble function of defects.

The ensemble function $g(T)$ before and after laser conditioning is calculated with the values of T_0, ΔT, and d listed in Table 1 using Eq. (2). The results are shown in Fig. 5.

In Fig. 5, $g(T)$ curve shifts to the right, toward a higher threshold of defects. The defects with lower threshold limits were removed from the ensemble curves. This indicates that the defects with lower threshold may be removed from the film or transformed to become defects with higher threshold. Some new defects with higher threshold should be produced during laser conditioning because the defect density is increased. We consider that the laser-conditioning effect depends on these two aspects. If removing the defects plays dominant role in the conditioning process, the increasing factor of threshold of the films could be larger. Otherwise, producing new defects would play a small but dominant role. When this exceeds the latter effect, the effects of laser conditioning do not emerge.

In conclusion, the effect of laser conditioning on ZrO_2/SiO_2 HR films at a wavelength of 1064 nm is studied with a small spot laser-conditioning scanning process using the method of fitting laser-induced damage probability curves. The results show that LIDT of the film could be increased by a factor of approximately 2.0. The influence of laser conditioning on the defects of the film is investigated by comparing the ensemble curve of defects before and after laser conditioning. Two aspects of laser conditioning on defects removal and new defects production are determined, and the effect of laser conditioning depends on their competition.

References

1. C. R. Wolfe, M. R. Kozlowski, J. H. Cambell, and F. Rainer, Proc. SPIE **1438,** 360 (1989).
2. M. R. Kozlowski, C. R. Wolfe, M. C. Staggs, and J. H. Cambell, Proc. SPIE **1438,** 376 (1989).
3. M. E. Frink, J. W. Arenberg, D. W. Mordaunt, S. C. Seitel, M. T. Babb, and E. A. Teppo, Appl. Phys. Lett. **51,** 415 (1987).
4. L. Sheehan, M. R. Kozlowski, F. Rainer, and M. C. Staggs, Proc. SPIE **2114,** 559 (1993).
5. E. Eva, K. Mann, N. Kaiser, B. Anton, R. Henking, D. Ristau, P. Weissbrodt, D. Mademann, L. Raupch, and E. Hacher, Appl. Opt. **35,** 5613 (1996).
6. Z.-X. Fan, Q. Zhao, H. Qiu, and R.-Y. Fan, Proc. SPIE **3244,** 469 (1998).
7. M. R. Kozlowski, M. C. Staggs, F. Rainer, and J. Stathis, Proc. SPIE **1441,** 269 (1990).
8. P. A. Temple, W. H. Lowdermilk, D. Milam, and G. Kennedy, Appl. Opt. **21**, 3249 (1982).
9. J. Huang, H. Lu, B. Ye, S. Zhao, H. Wang, X. Jiang, X. Yuan, and W. Zheng, Chinese J. Lasers (in Chinese) **34,** 723 (2007).
10. X. Liu, D. Li, X. Li, Y. Zhao, and J. Shao, Chinese J. Lasers (in Chinese) **36,** 1545 (2009).
11. D. Li, Y. Zhao, J. Shao, Z. Fan, and H. He, Chin. Opt. Lett. **6,** 386 (2008).
12. N. Bloembergeb, Appl. Opt. **12,** 661 (1972).
13. L. G. Deshazer, B. E. Newnam, and K. M. Leung, Appl. Phys. Lett. **23,** 607 (1973).
14. H. Krol, L. Gallais, C. Grezes-Besset, J.-Y. Natoli, and M. Commandre, Opt. Commun. **256,** 184 (2005).
15. J. Capoulade, L. Gallais, J.-Y. Natoli, and M. Commandré, Appl. Opt. **47,** 5272 (2008).
16. J. O. Porteus and S. C. Seitel, Appl. Opt. **23,** 3796 (1984).
17. R. M. O'Connell, Appl. Opt. **31,** 4143 (1992).
18. J. Y. Natoli, L. Gallais, H. Akhouayri, and C. Amra, Appl. Opt. **41,** 3156 (2002).
19. ISO standard 11254-1, "Determination of laser-damage threshold of optical surfaces—part 1: 1-on-1 test" (2000).